2021 43rd Annual International Conference of the
IEEE Engineering in Medicine & Biology Society (EMBC)
Oct 31 - Nov 4, 2021. Virtual Conference

Modeling the Dielectrophoretic Separation of Red Blood Cells (RBCs) from B-Lymphocytes (B-Cells) *

Osman Sahin[1], Ali Kosar [1,2,3 †], Murat Kaya Yapici [1,2,3,4 † *], †*Member, IEEE*

***Abstract*— The ability to characterize hematopoietic cells quickly and reliably is critical in precision medicine. Analysis of hematopoietic cells will lead to the diagnosis of various diseases, including infectious diseases and cancer. Microfluidic devices provide label-free, time-efficient, and quantitative analysis in this regard. A microfluidic system is provided in this work to separate Red blood cells (RBCs) from B-Lymphocytes (B-Cells). One of the ways for manipulating and separating micron-sized particles is dielectrophoresis (DEP). Dielectrophoretic manipulation of red blood cells (RBC) and B-Lymphocytes (B-Cells), with diameters of 2.8 µm and 3.29 µm, respectively, is studied. The simulation results of a microfluidic device with a sidewall electrode are shown. RBCs could be separated with 98 % efficiency from B-Cells at an applied voltage ±0.06 V with a frequency and flow rate of 10 kHz and 1.5 µL/s, respectively.**

I. INTRODUCTION

The advances in microfluidic devices regarding particle separation and manipulation have played a significant role in biological sample processing for early and rapid detection [1]. Blood consisting of hematopoietic cells serves as a sample fluid for diagnosing various diseases, including infectious diseases and cancer [2]. Hematopoietic stem cells provide the production of blood cells employing red and white blood cells. In a conventional laboratory, to detect pathogen-related illnesses from the blood, many processes are required because of extensive and time-consuming laboratory equipment [1]. However, with the emergence of microfluidic technologies, miniaturized devices have been preferred due to portability and shorter assay time [1]. The miniaturized devices provide many advantages including time-efficiency, quick response to the reaction process, lower fabrication cost [3].

One of the most well-known methods for separating small particles is dielectrophoresis (DEP) [4]. A dielectrophoretic force occurs when cells are subjected to a non-uniform electric field. Depending on the polarizability of the medium and particle, the particle can be repelled or attracted.

In microfluidic systems, DEP is a method to be employed for many micro/nanoscale bio-particles (i.e., virus, DNA, blood, bacteria) [5]. It can also be performed in many microfluidic applications, such as in separation and sorting [6-8], particle trapping [9-10]. Various applications of DEP for separation in blood samples have been already realized. For instance, Pommer, Matthew S., et al. [11] used a microfluidic channel to extract platelets from diluted blood samples. They used size differences between platelets and blood cells to separate them. Gascoyne, PR, et al [12] used DEP force to separate viable cultured breast tumor cells from peripheral blood.

In this study, for the separation of RBCs, a DEP-based microfluidic device is modeled. In this approach, RBCs are separated from B-cells and are directed to the bottom or top side of the outlet reservoir based on the frequency. Differences in dielectric properties make it possible to occur efficient separation in addition to differences in frequency response. The effects of different parameters including frequency and voltage values as well as the size of the electrodes are displayed by simulating in the commercial software COMSOL 5.3.

II. THEORY

The dielectric characteristics of particles with varying polarizability and permittivity affect DEP [13]. Depending on the permittivity of particles and their surrounding medium, particles could be directed in different directions. The DEP force is expressed as follow;

$$F_{DEP} = 2\pi\varepsilon_m r^3 \mathrm{Re}\left\{\frac{\varepsilon^*_{eff} - \varepsilon^*_m}{\varepsilon^*_{eff} + 2\varepsilon^*_m}\right\} \nabla E^2_{RMS}$$

The dielectrophoretic force depends on the permittivity of the medium ε_m, the radius of cell r, the real part of the Clausius-Mossotti factor f_{cm} and the exposed non-uniform electric field E. The real part of the Clausius-Mossotti factor f_{cm} is given as follow;

$$f_{cm}(w) = \frac{\varepsilon^*_{eff} - \varepsilon^*_m}{\varepsilon^*_{eff} + 2\varepsilon^*_m}$$

$\varepsilon^* = \varepsilon - j(\frac{\sigma}{w})$ is the complex permittivity where w is applied frequency, and σ is the electrical conductivity. Based on the single-shell model, ε^*_{eff} is formulated as follow;

$$\varepsilon^*_{eff} = \varepsilon^*_m \frac{(\frac{r}{r-d})^3 + 2\frac{\varepsilon^*(int) - \varepsilon^*(mem)}{\varepsilon^*(int) + 2\varepsilon^*(mem)}}{(\frac{r}{r-d})^3 - \frac{\varepsilon^*(int) - \varepsilon^*(mem)}{\varepsilon^*(int) + 2\varepsilon^*(mem)}}$$

where the thickness of the cellular membrane (d), the complex permittivity of the cytoplasm (ε^*_{int}) and complex permittivity of the membrane (ε^*_{mem}). When ε^*_m the complex permittivity of the medium is less than ε^*_{eff} the complex permittivity of the cell, $f_{cm}(w)$ will be positive. Otherwise, it will be a negative value. The value of Re $\{f_{cm}(w)\}$ is

1 Faculty of Engineering and Natural Sciences, Sabanci University, Istanbul 34956, Turkey (e-mail: osahin@sabanciuniv.edu)

2 Sabanci University Nanotechnology and Application Center, Sabanci University, Istanbul 34956, Turkey (e-mail: ali.kosar@sabanciuniv.edu)

3 Center of Excellence for Functional Surfaces and Interfaces for Nano-Diagnostics, Sabanci University, Istanbul, TR

4 Department of Electrical Engineering, University of Washington, Seattle, WA 98195, USA (* mkyapici@sabanciuniv.edu)

changeable between -1/2 and 1 and is related to frequencies of the electrical field applied.

Table 1 lists the most important characteristics for fluid and particles which are assumed to have a spherical geometry.

Table 1 Particle Parameters of B-cell and RBC [2]

Fluid	Permittivity	80
	Viscosity	8.94e-4 Pa*s
	Density	1000 kg/m^3
	Conductivity	0.01 S/m
RBC	Diameter	2.8 um
	Permittivity	59
	Shell Permittivity	4.44
	Density	1050 kg/m^3
	Conductivity	0.31 S/m
	Shell Conductivity	1e-6 S/m
	Shell Thickness	4.5 nm
B-Cell	Diameter	3.29 um
	Permittivity	154.4
	Shell Permittivity	10.67
	Density	1050 kg/m^3
	Conductivity	0.73 S/m
	Shell Conductivity	5.6e-5 S/m
	Shell Thickness	7.5 nm

Using the polarizability difference of RBC and B-cell, the graph of Clausius-Mossotti factors plotted by a MATLAB script is illustrated in Fig.1

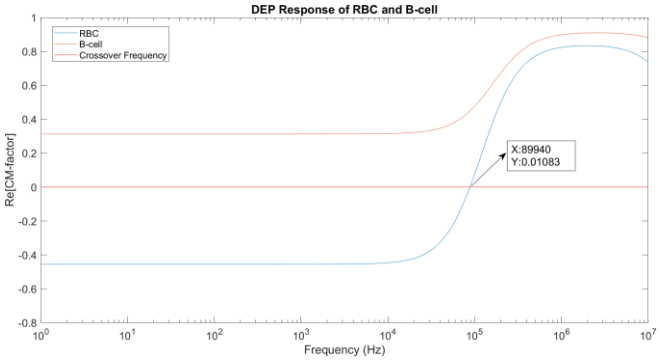

Figure 1. Real Part of Clausius-Mossotti factor for RBC and B-cell

III. FINITE ELEMENT MODELLING

In this study, the 2D model was modeled depending on the COMSOL Multiphysics software tool. To perform the dielectrophoretic separation of particles in the aqueous solution, fluid flow was used in the microfluidic channel with a single inlet and two outlets. The array of the electrode was considered to create a non-uniform electrical field. In the microfluidic channel, three parts were formed in the channel: injection, separation, collection regions. Two particles, RBCs, and B-cells entered the inlet at a flow rate of 1.5 µL/s. The domain is illustrated in Fig 2.

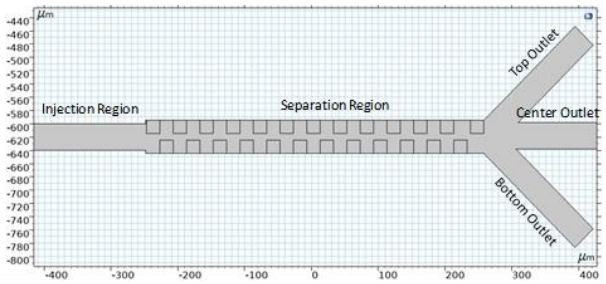

Figure 2. The geometry of the simulated module

Because the aqueous solution was non-Newtonian, the Creeping Flow (spf) module was used to describe the fluid flow along the channel. Navier-stokes equation determines fluid flow within the channel

$$0 = \nabla \cdot [-\mathrm{pl} + \mu(\nabla u + (\nabla u)^T)] + F$$

$$\nabla.(\mathrm{pu}) = 0$$

where p is the pressure, u is the velocity vector, µ is the dynamic viscosity and F is the volume force vector. Initial fluid velocity was applied at the inlet and the output was arranged to zero fluid velocity [14]. The wall conditions were imposed using the non-slip condition.

The Electric Currents (ec) module was used to simulate the electric field in the microchannel, which was affected by the electric potential (v) applied to the electrode set. As physical interfaces, the Particle Tracing for Fluid Flow module (fpt) was used to compute the trajectories of RBCs and B-cells under the effect of drag and dielectrophoretic forces. Drag force is one of the forces caused by fluid flow. Brownian and motion and the gravity force were ignored.

IV. DEVICE DESIGN

To create a non-uniform electric field, a group of electrodes is needed to apply an electrical voltage. Taking into consideration the DEP force formula, it can be seen that when a higher electric field gradient across an electrode is observed, the strength of dielectrophoresis will be more so that particles can be oriented to the output more easily [13]. A non-uniform electric field is created between two groups of electrodes facing each other. Because DEP includes the non-uniform electric fields, the changes in the value of the electric field caused by the differences in electrode geometry have an important effect on the behavior of the particles.

The gradient of the electric field depends on various parameters such as the distance between electrodes in the same row or column [15]. To observe the intensity differences for the electric field gradients, simulations for different designs were performed as illustrated in Fig.3. The literature and simulation results were agreed that fingered electrodes resulted in a higher electrical field across a set of electrodes due to a higher field gradient compared to fingerless electrodes [13].

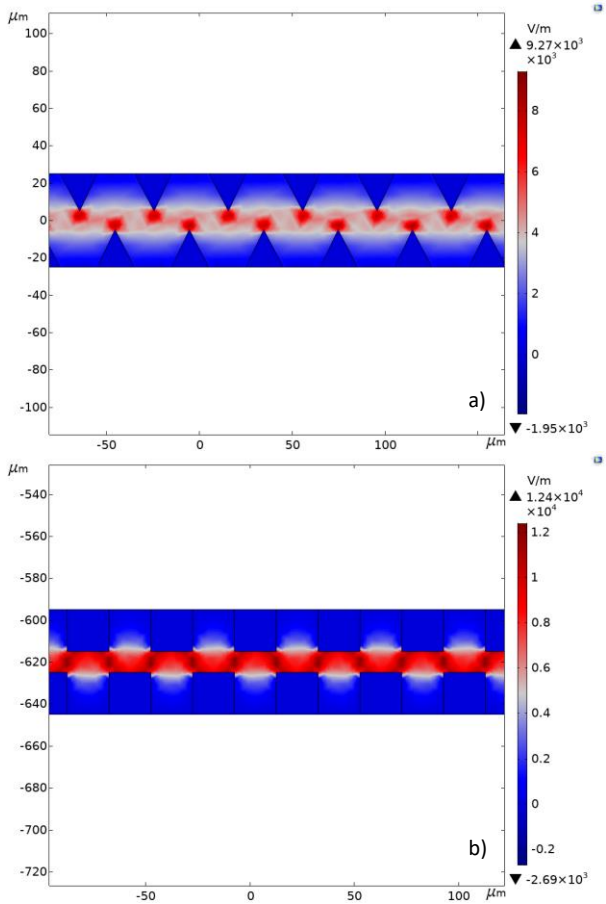

Figure 3. Surface electric field for a) fingerless and b) fingered electrodes

V. RESULTS

Particles show the same behaviors and go through the center of the outlet without activating the DEP force module. On the other hand, with the DEP force module, the particles entering the channel are affected by drag and dielectrophoresis forces depending on applied frequency, the value of voltage, and the permittivity of the medium and particles. In each particle trajectory graph, there are two types of color bars representing surface electric field and radius of B-cell and RBC, consecutively.

In Fig.4a, RBCs, and B-cells were directed to the same outlet without separation for ±0.01 V at 10 kHz. However, when the voltage was arranged for the bottom and top electrode at ± 0.06 V at 10 kHz, the separation occurs as shown in Fig 4b. On the other hand, Fig.4c demonstrates the effect of frequency change from 10 kHz to 100 kHz which RBCs deviate to a different outlet based on frequency response.

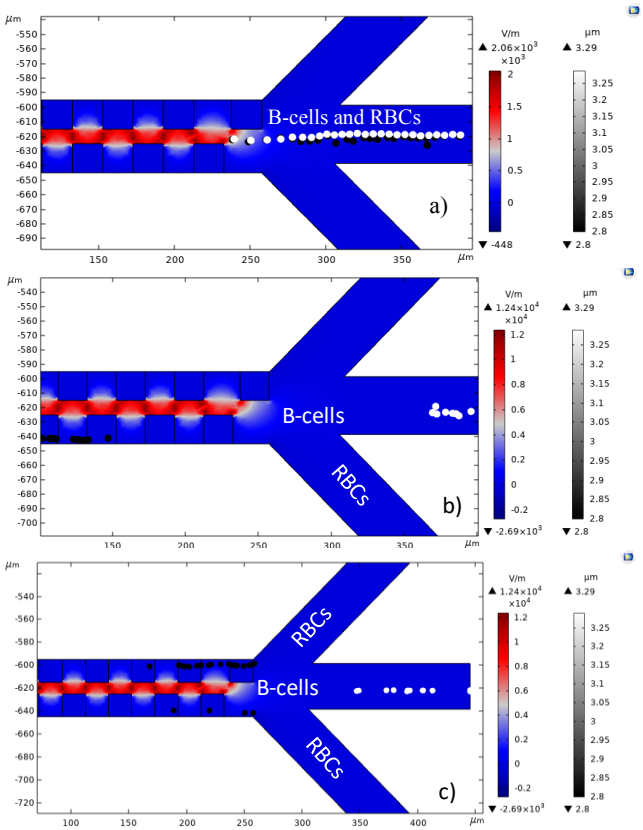

Figure 4. Applied voltage for a) V = ±0.01 V at 10 kHz, no separation occurs, b) V = ± 0.06 V at 10 kHz, c) V = ±0.06 V at 100 kHz separation occur, but on different direction.

Fig.5 illustrates the separation efficiency arranging for ±0.06 V at 10 and 100 kHz. By setting the simulation time, 55 total particles were released. At 10 kHz, approximately all RBC cells were guided to the bottom outlet as seen in Fig. 5a. However, at 100 kHz, Fig. 5b demonstrates that collection efficiency decreases to 80 %.

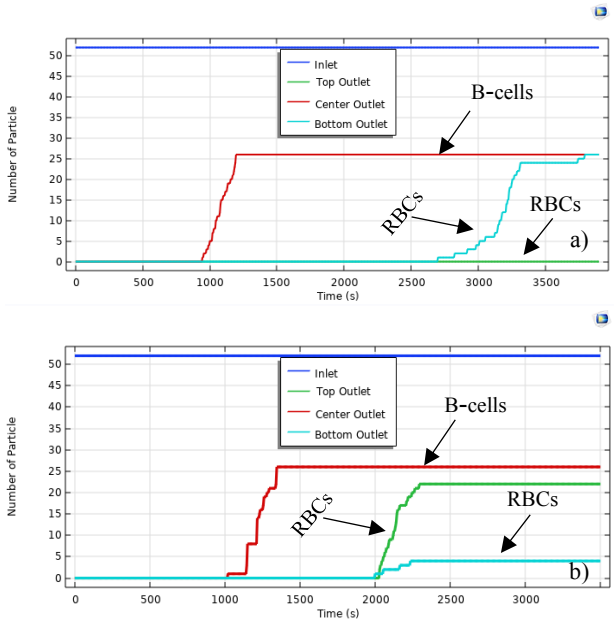

Figure 5. The efficiency of separation for a) 10 kHz and b) 100 kHz

The length of the gap between electrodes placed in the same row is another parameter for change the strength of the electric field. In the case of the length of 10 µm, as shown in Fig 6a, the strength of the electric field is increased in comparison to a length of 30 µm in Fig.6b

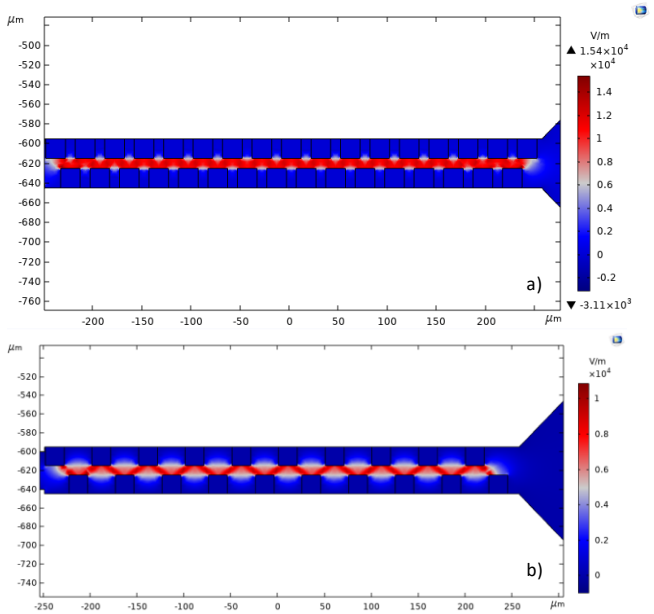

Figure 6. Comparison for the length of the electrode gap for a) 10 and b) 30 µm

The height of the electrodes leads to changes in the electric field intensity. To demonstrate that effect, Fig. 7a shows the result of the height of electrodes 10 µm. Compared to 22.5 µm height as seen in Fig.7b, the intensity of the electric field decreases.

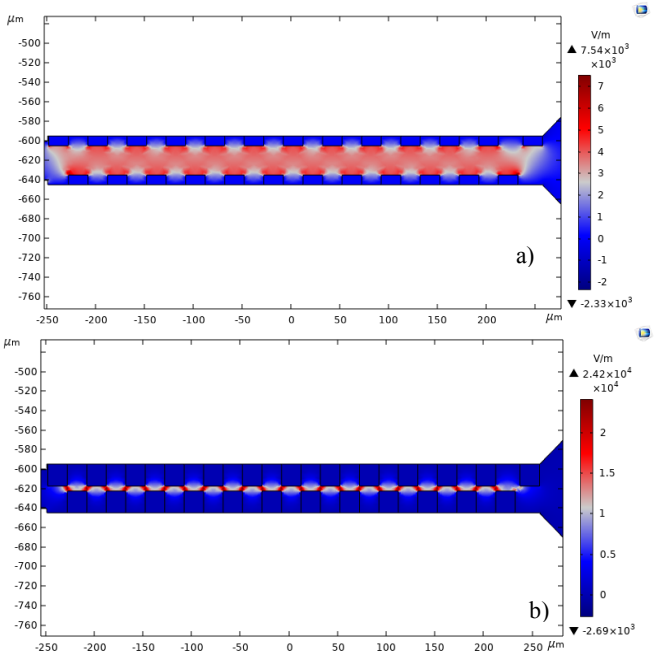

Figure 7. Increase in height of electrode from a) 10 to b) 22.5 µm

VI. Conclusion

This study presents microfluidic device simulations for separating red blood cells (RBCs) from B-Lymphocytes (B-Cells) according to their dielectric responses at different frequencies. At 10 kHz or 100 kHz, both particles could be separated at different outlets based on their Clausius-Mossotti factors. Also, it can be seen that the value of voltage is one of the significant effects when its value becomes enough to activate their separation. Because the electric field gradient is inversely proportional to the distance between electrodes, the intensity of the electric field diminishes as the gap length between electrodes increases. Finally, the height of the electrode is proportional to the strength of the electric field due to an increase in electric field penetration between the electrodes.

Acknowledges

This project was supported by The Scientific and Technological Research Council of Turkey (TUBITAK) grant number 218S893.

References

[1] Park, Seungkyung, et al. "Continuous dielectrophoretic bacterial separation and concentration from physiological media of high conductivity." Lab on a Chip 11.17 (2011): 2893-2900.

[2] Erdem, Nurdan, Yağmur Yıldızhan, and Meltem Elitaş. "A numerical approach for dielectrophoretic characterization and separation of human hematopoietic cells." International Journal of Engineering Research & Technology (IJERT) 6.4 (2017): 1079-1082.

[3] Li, Ming, et al. "A review of microfabrication techniques and dielectrophoretic microdevices for particle manipulation and separation." *Journal of Physics D: Applied Physics* 47.6 (2014): 063001.

[4]Khoshmanesh, Khashayar, et al. "Dielectrophoretic platforms for bio-microfluidic systems." Biosensors and Bioelectronics 26.5 (2011): 1800-1814.

[5] Qian, Cheng, et al. "Dielectrophoresis for bioparticle manipulation." International journal of molecular sciences 15.10 (2014): 18281-18309.

[6] Piacentini, Niccolò, et al. "Separation of platelets from other blood cells in continuous-flow by dielectrophoresis field-flow-fractionation." *Biomicrofluidics* 5.3 (2011): 034122.

[7] Zhang, Chen, et al. "Dielectrophoretic separation of carbon nanotubes and polystyrene microparticles." Microfluidics and nanofluidics 7.5 (2009): 633.

[8] Demierre, Nicolas, et al. "Focusing and continuous separation of cells in a microfluidic device using lateral dielectrophoresis." Sensors and Actuators B: Chemical 132.2 (2008): 388-396.

[9] Xiong, Xugang, et al. "Directed assembly of gold nanoparticle nanowires and networks for nanodevices." Applied Physics Letters 91.6 (2007): 063101.

[10] Asbury, Charles L., Alan H. Diercks, and Ger Van Den Engh. "Trapping of DNA by dielectrophoresis." *Electrophoresis* 23.16 (2002): 2658-2666.

[11] Pommer, Matthew S., et al. "Dielectrophoretic separation of platelets from diluted whole blood in microfluidic channels." *Electrophoresis* 29.6 (2008)

[12] Gascoyne, Peter RC, and Sangjo Shim. "Isolation of circulating tumor cells by dielectrophoresis." Cancers 6.1 (2014): 545-579.

[13] Uran, Can. Fabrication of an on-chip nanowire device with controllable nanogap for manipulation, capturing, and electrical characterization of nanoparticles. Diss. Bilkent University, 2008.

[14] Ettehad, Honeyeh Matbaechi, Subhajit Guha, and Christian Wenger. "Simulation of CMOS compatible sensor structures for dielectrophoretic biomolecule immobilization." *COMSOL Conference, Rotterdam, Netherlands*. 2017.

[15] Sadeghian, Hesam, Yousef Hojjat, and Masoud Soleimani. "Interdigitated electrode design and optimization for dielectrophoresis cell separation actuators." Journal of Electrostatics 86 (2017): 41-49.